PROCEEDINGS OF SCIENCE

Identified-particle production and spectra with the ALICE detector in pp and Pb–Pb collisions at the LHC

S.Beolè[*†]
Università di Torino and INFN
E-mail: beole@to.infn.it

Thanks to its unique capabilities the ALICE experiment can measure the production of identified particles over a wide momentum range both in pp and Pb–Pb collisions at the LHC. In this report, the particle-identification (PID) detectors and techniques as well as the performance achieved are shortly reviewed. The particle identification of the Inner Tracking System (ITS) and the Time Projection Chamber (TPC) are based on the specific energy loss whereas the Time-Of-Flight detector (TOF) determines the particle velocity by measuring its flight time. The current results on hadron transverse momentum spectra measured in proton–proton (pp) collisions at $\sqrt{s} = 900$ GeV and 7 TeV, and in Pb–Pb collisions at $\sqrt{s_{NN}} = 2.76$ TeV are shown. In particular, pp results on particle production yields, spectral shapes and particle ratios are presented as a function of the collision energy and compared to previous experiments and commonly-used Monte Carlo models. Particle spectra, yields and ratios in Pb–Pb are measured as a function of the collision centrality and the results are compared with published RHIC data in Au–Au collisions at $\sqrt{s_{NN}} = 200$ GeV and predictions for the LHC.

50th International Winter Meeting on Nuclear Physics - Bormio2012,
23-27 January 2012
Bormio, Italy

[*]Speaker.
[†]for the ALICE collaboration

PoS(Bormio2012)051

1. Introduction

ALICE (A Large Ion Collider Experiment) is the only experiment at the CERN LHC (Large Hadron Collider) specifically designed to study the physics of strongly-interacting matter and the quark–gluon plasma in heavy–ion collisions. The ALICE detector combines many different detector technologies as shown in Fig. 1. ALICE was designed to fulfill challenging requirements both on tracking and particle-identification as extensively detailed in [4]. Thanks to these features, the experiment is able to identify charged hadrons in a wide momentum range extending from about 0.1 GeV/c and up to several GeV/c by combining different detecting systems. The hot and dense matter produced in ultra–relativistic heavy–ion collisions evolves through different phases to a freeze-out where strong interactions among the hadrons stop [1]. Since produced hadrons carry information about the evolution of the system, the measurement of the transverse momentum distributions and yields of identified hadrons is essential to understand the global properties and dynamics of the later stages [2]. Preliminary results on charged-hadron spectra and yields at mid-rapidity are presented both for pp collisions at $\sqrt{s} = 0.9$ and 7 TeV and Pb–Pb collisions at $\sqrt{s_{NN}} = 2.76$ TeV. Final results will be published in the next months on a specialized journal. A comprehensive review of all the ALICE recent results can be found in [3].

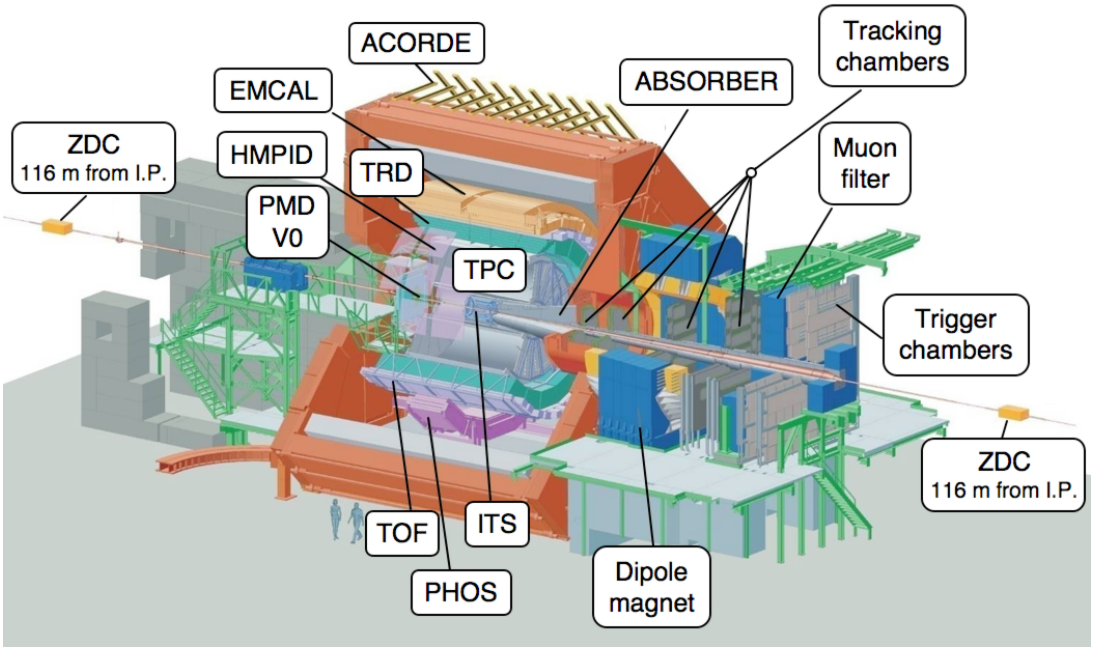

Figure 1: Schematic view of the ALICE detector.

2. Particle Identification with the ALICE detector

In this section, the particle-identification (PID) detectors relevant for this analysis are briefly discussed, namely the Inner Tracking System (ITS), the Time Projection Chamber (TPC) and the

Time-Of-Flight detector (TOF). A detailed review of the ALICE detector and of its PID capabilities can be found in [5]. The Inner Tracking System (ITS) of the ALICE experiment consists of six cylindrical layers of silicon detectors. Each layer is coaxial with the beam–pipe and has hermetic structure. The ITS covers the pseudo–rapidity range $|\eta| \leq 0.9$ (η= -ln tan $\theta/2$, with θ being the polar angle) and the distance from the nominal beam line ranges from 3.9 cm for the innermost layer up to 43 cm for the outermost. The two innermost layers are made of Silicon Pixel Detectors (SPD), the two central layers of Silicon Drift Detectors (SDD) and the two outermost layers of double sided Silicon Strip Detectors (SSD). In total the ITS has $\approx$ 12.5M read–out channels.
The ITS is able to reconstruct both primary and secondary interaction points and constrains the ALICE central barrel tracks in the vicinity of the interaction point which enables rejection of secondary tracks. Furthermore, as a standalone tracker, the ITS measures particles which do not reach or are missed by the external barrel detector, due to acceptance limitations and momentum cutoff. The particle identification in the Inner Tracking System (ITS) is based on the measured energy deposit per unit length of a track, denoted dE/dx hereafter. Silicon Drift Detectors (SDD) and Silicon Strip Detectors (SSD) provide analogue read–out for up to four samples for a truncated mean calculation of the dE/dx. Thus a resolution of $\sigma_{dE/dx}$=10–15% is achieved (see Fig. 2 left panel). The particle identification in the ITS combined with stand-alone tracking allows to identify pions with a minimum momentum of $p_T \approx 100$ MeV/c which reduces the systematic error introduced by the extrapolation of the yield and $\langle p_T \rangle$ measurements to $p_T = 0$. The TPC is the main central-barrel tracking detector of ALICE, covering the pseudo–rapidity range $|\eta| \leq 0.9$. With its 557 568 readout channels it provides up to 159 ionization samples in a gas mixture of Ne, CO_2, N_2 (85.7% – 9.5% – 4.8%) at atmospheric pressure. A truncated mean is used to reduce the Landau tail resulting in a Gaussian distribution with a resolution of $\sigma_{dE/dx} \approx 5\%$. Figure 2, right panel, shows the measured dE/dx versus the track momentum p. The lines show a parameterization of the Bethe–Bloch curve. With the measured particle momentum and $\langle dE/dx \rangle$ the particle type can be determined by comparing the measurements against the Bethe-Bloch expectation.

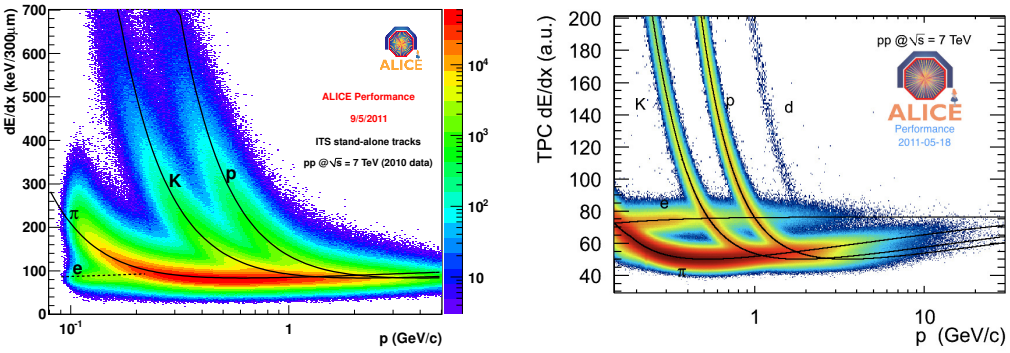

Figure 2: dE/dx as a function of particle momentum measured in the ITS (left) and TPC (right) in pp collisions at $\sqrt{s} = 7$ TeV.

The TOF detector is a large-area array of 1638 Multigap-Resistive Plate Chambers (RPC) and covers the central pseudo–rapidity region ($|\eta| < 0.9$, full azimuth). The TOF RPCs pro-

vide an intrinsic time resolution of approximately 50 ps. The overall time resolution for particle identification also depends on the time-0 uncertainty of the event. This results in a resolution of $\sigma_{TOF} = \sqrt{\sigma^2_{intr} + \sigma^2_{t0}} \approx 86$ ps for Pb–Pb collisions and $\sigma_{TOF} \approx 120$ ps for pp collisions, the difference being due to the different number of tracks used to determine the time-0 in the different collisions. Particle identification is performed by matching momentum and trajectory-length measurements obtained with the tracking system to the time–of–flight information provided by the TOF system, as shown in Fig. 3, left panel. In central Pb–Pb collisions, some tracks are uncorrectly associated with a TOF signal resulting in the background visible in Fig. 3, left panel. The TOF signal distribution is then fitted for each p_T bin with data-derived templates for different particle species allowing to extract the particle yields when the separation is as low as 2σ, as shown in Fig. 3, right panel. From the plot one can see that pions and kaons can be separated up to ≈ 3GeV/c while protons and kaons can be separated up to ≈ 5 GeV/c.

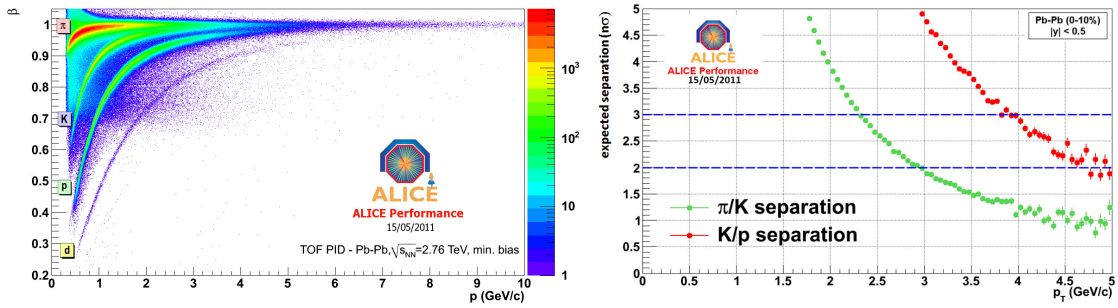

Figure 3: Track velocity β vs. momentum p (left) and π/K and K/p separation for the Time Of Flight detector.

Particles can also be identified in ALICE with topological identification or invariant mass fits. This is the case for weak decays, resonances and kaon decays ("kinks"), where PID detectors can be used to improve the signal over background ratio, without any loss of the actual signal, by means of "compatibility cuts" with the PID signal (e.g. requiring that the dE/dx signals of the kaons in a $\phi \to$ KK candidate are within 3 sigma of the expected average value).

3. Results in pp collisions at $\sqrt{s} = 0.9$ and 7 TeV

The transverse momentum spectra of primary π, K and p are measured at mid-rapidity (|y| < 0.5) combining the techniques and detectors described in the previous section. Data are normalized to the number of inelastic collision N_{inel} as described in [7]. Primary particles are defined as prompt particles produced in the collision and all decay products, except products from weak decay of strange particles. The contribution from the feed-down of weakly-decaying particles to π and p and from protons from material are subtracted by fitting the data using Monte Carlo templates of the distance of closest approach, DCA, distributions. In this section we present results for π, K, p measured in pp collisions at $\sqrt{s} = 7$ TeV. In Fig. 4 the transverse momentum spectra, fitted by a Levy-Tsallis [6] function, are shown for π, K and p, both for positive (left) and negative (right) particles. The fit with the Levy-Tsallis function is used to extrapolate down to $p_T = 0$ and to extract the average p_T for each particle species. The data can be compared to existing measurements at lower energy, in particular published ALICE results at $\sqrt{s} = 0.9$ TeV [7].

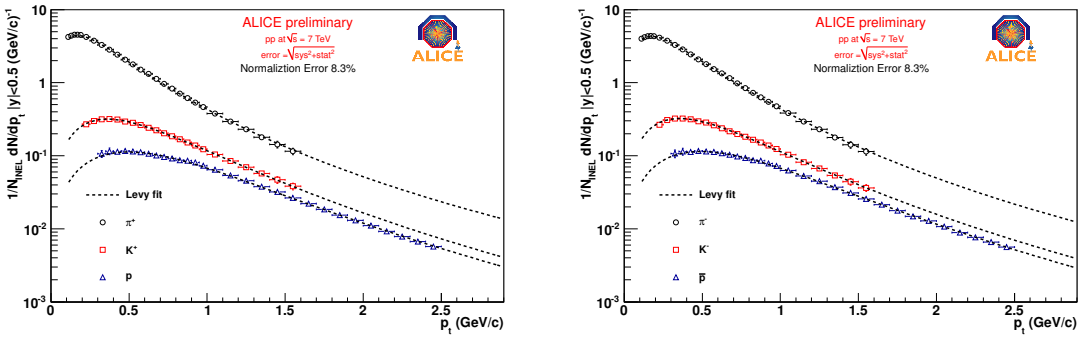

Figure 4: Transverse momentum spectra for positive (left panel) and negative (right panel) identified particles (π, K, p) at $\sqrt{s} = 7$ TeV

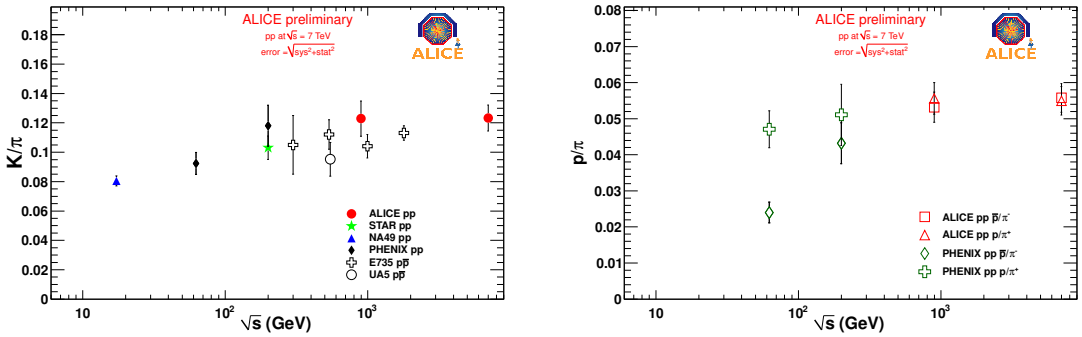

Figure 5: $(K^+ + K^-)\,/(\pi^+ + \pi^-)$ (left panel) and p/π^+, $\bar{p}/\pi^-$ (right panel) as a function of $\sqrt{s}$

As it can be seen in Fig. 5, the K/π ratio is rather independent of energy, at least starting from RHIC energies ($\sqrt{s_{NN}} = 200$ GeV), despite the large increase in the center of mass energy. The p/π ratio is shown for separate charges in the right panel. The difference between the two charges at $\sqrt{s_{NN}} = 200$ GeV reflects the baryon/antibaryon asymmetry, which essentially vanishes at LHC energies as already reported in [8], leading to a constant value of about 0.05 for the two sets of data at the two different energies measured by ALICE.

4. Results in Pb–Pb collisions at $\sqrt{s_{NN}} = 2.76$ TeV

The spectra of π, K and p were measured using a combined ITS, TPC and TOF analysis, similarly to what was done in pp, in several centrality classes (see [9] for details on centrality selection) from 100 MeV/c up to 3 GeV/c for pions, from 200 MeV/c up to 2.0 GeV/c for kaons and from 300 MeV/c up to 3 GeV/c for protons and antiprotons. Individual fits to the data to extrapolate the spectra outside the measured p_T range are performed following the blast-wave model parameterization [10]. The measured spectra and corresponding fits are shown in Fig. 6 for positive particles in different centrality bins. Average transverse momenta $\langle p_T \rangle$ and integrated production yields dN/dy are obtained using the measured data points and the extrapolation.

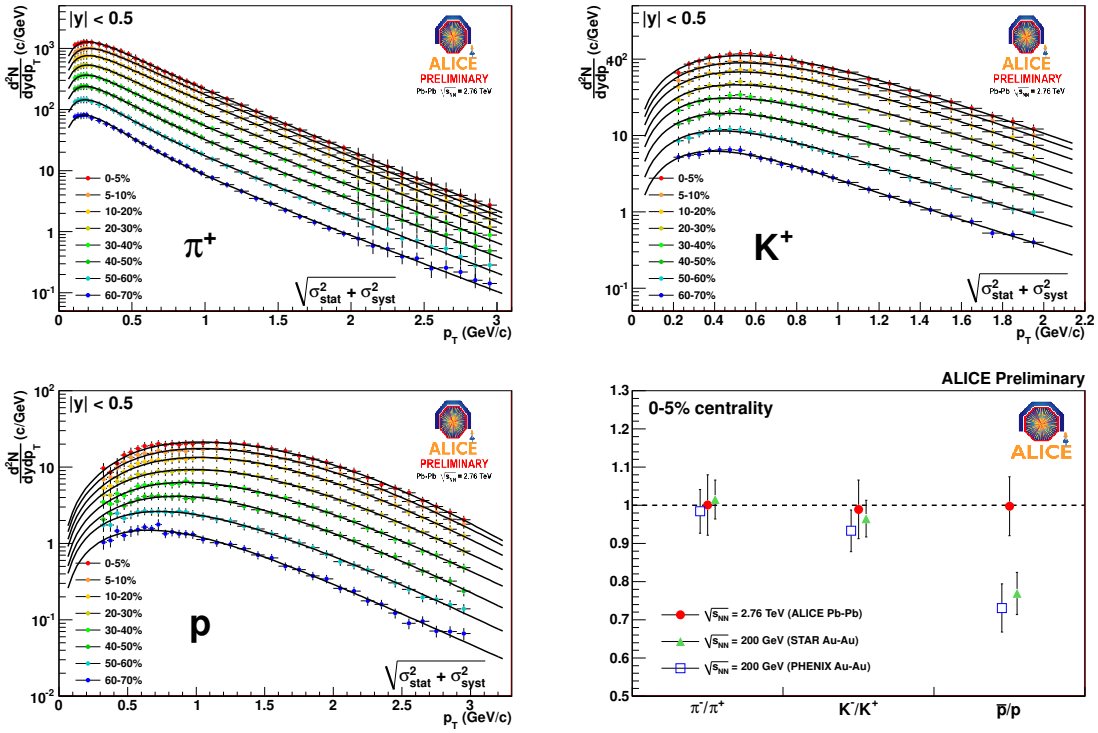

Figure 6: Transverse momentum spectra of primary π (top left), K (top right), p (bottom left) and corresponding fits in Pb–Pb collisions at $\sqrt{s} = 2.76$ TeV. Bottom right: anti–particle/particle ratio for different species for central collisions compared to RHIC data.

Antiparticle/particle ratios consistent with unity for all particle species in all centralities (see Fig. 6 bottom right) suggest that the baryo-chemical potential μ_B is close to zero as expected at LHC energies. The p_T-integrated K^-/π^- and $\bar{p}/\pi^-$ ratios are shown in Fig. 7 as a function of the charged-particle density $dN_{ch}/d\eta$ [9] and are compared with RHIC data at $\sqrt{s_{NN}}$ = 200 GeV [14, 15, 16] and ALICE proton-proton results at $\sqrt{s} = 7$ TeV [11]. The K^-/π^- production trend is compatible to the one measured by STAR. The $\bar{p}/\pi^-$ results are similar to previous measurements performed by PHENIX and BRAHMS whose feed–down subtraction for protons is close to ours. Proton measurements reported by STAR are inclusive. Finally, the $\bar{p}/\pi^-$ ratio measured at the LHC (≈ 0.05) is significantly lower than the value expected from statistical model predictions ($\approx 0.07 - 0.09$) with a chemical freeze-out temperature of $T_{ch} = 160 - 170$ MeV at the LHC [12, 13]. The measured hadron $\langle p_T \rangle$ are shown in Fig. 8 (left panel) as a function of $dN_{ch}/d\eta$ for π^-, K^- and $\bar{p}$ and are compared to STAR results in Au–Au collisions at $\sqrt{s}$ = 200 GeV. The spectra are observed to be harder than those at RHIC for similar $dN_{ch}/d\eta$. To give a quantitative estimate of the thermal freeze-out temperature T_{fo} and of the average transverse flow $\langle \beta \rangle$, a detailed study of the spectral shapes has been done. We performed a combined blast-wave fit of the spectra (the model description can be found in [10]) in the ranges 0.3-1.0 GeV/c for pions, 0.2-1.5 GeV/c for kaons and 0.3-3.0 GeV/c for protons. The T_{fo} parameter is slightly sensitive to the pion fit range because of feed-down of resonances, while the transverse flow measurement is not, being dominated by the proton spectral shape.

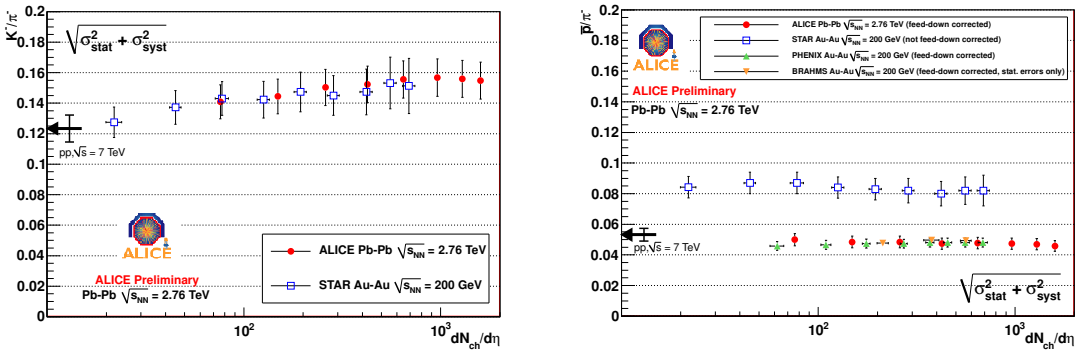

Figure 7: K^-/π^- (left panel) and $\bar{p}/\pi^-$ (right panel) production ratios as a function of $dN_{ch}/d\eta$ compared to RHIC data.

The results obtained on T_{fo} and for the average transverse flow $\langle\beta\rangle$ in different centrality bins are compared to the results of similar measurements performed by the STAR Collaboration at lower energies and shown in Fig. 8. As expected from the observation of the spectra, stronger radial flow is found with respect to RHIC, being about 10% larger in the most central collisions at the LHC.

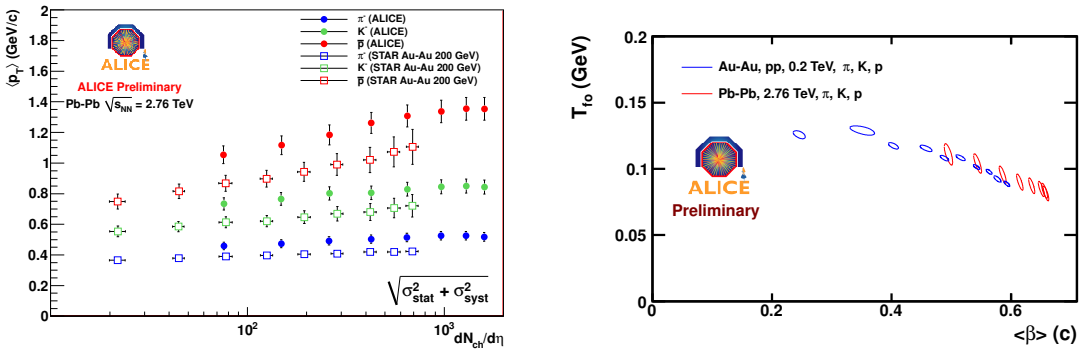

Figure 8: Left: mean p_T as a function of $dN_{ch}/d\eta$ for π, K and p compared to RHIC data. Right: Thermal freeze-out parameters T_{fo} and $\langle\beta\rangle$ from combined blast-wave fits compared to RHIC data.

Focusing our attention to the $0-5\%$ most central collisions, we can also compare our results to previous ones obtained at RHIC at $\sqrt{s_{NN}} = 200$ GeV [14, 15], as shown in the left panel of Fig. 9. In order to extend the p_T range for kaons, also the K^0_S spectra are shown on the same plot. The ALICE results refer to primary particles as described in the previous section, i.e. feed-down from weak decays are subtracted. At RHIC the situation is not always homogeneous: the (anti)protons from PHENIX are corrected for feed-down, while the ones from STAR are usually not. For this reason, only $\bar{p}$ from PHENIX are shown in Fig. 9 (left panel). On the other hand, the π from PHENIX are not corrected for feed-down, but since this is a much smaller correction than in the case of (anti)protons, also these data are presented in the figure. An evident change in the spectral shape is observed, with those measured at the LHC being much flatter at low p_T and harder, indicating a much stronger radial flow. The data were also compared to a hydrodynamical prediction [18]. While the model is able to reproduce the gross features of the π and K distributions,

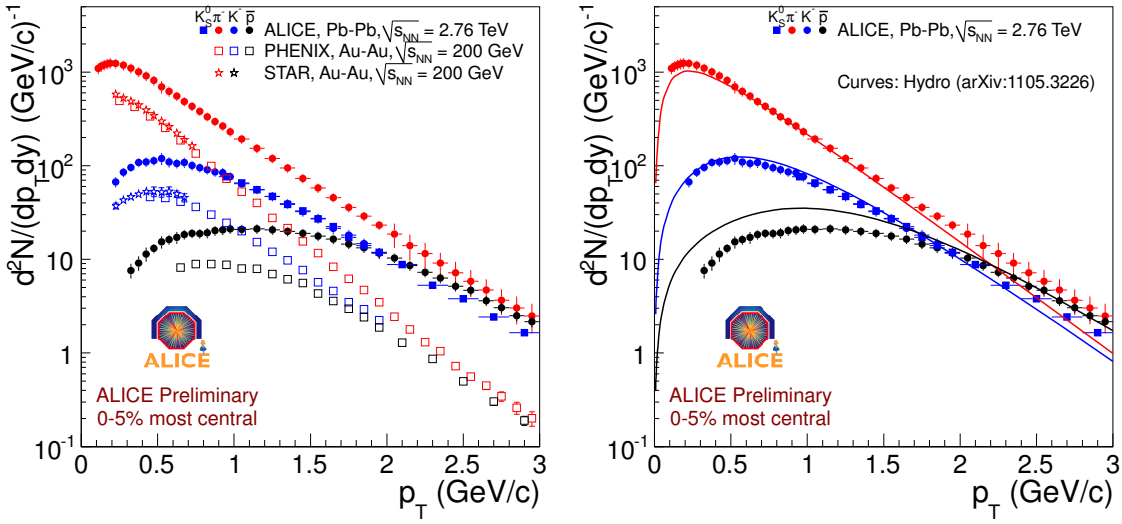

Figure 9: Spectra in the $0-5\%$ most central bin, compared to previous results at lower energy (left panel) and to the prediction from a hybrid hydrodynamical model (right panel).

it strongly disagrees with the measured p spectrum, both in shape and yield, as visible in Fig. 9 (right panel) and already reported in [17]. A similar disagreement was observed when comparing proton elliptic v_2 to the same model [19]. The difference in shape indicates a much stronger radial flow in the data than expected from the model, which could be partially due to extra flow built up in the hadronic phase [20]. The difference in the proton yield can be ascribed to the fact that the model derives yields from a thermal model assuming $T_{ch} = 165$ MeV.

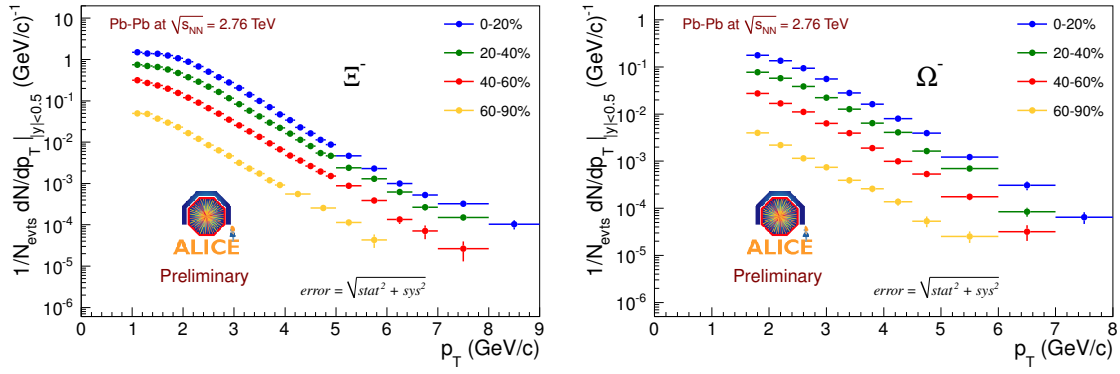

Figure 10: Transverse momentum spectra in PbPb at $\sqrt{s_{NN}} = 2.76$ TeV for different centrality samples for Ξ^- (left panel) and Ω^- (right panel).

The multi-strange baryons were measured via the topological identification of the decay channels $\Xi \to \Lambda + \pi \to p + \pi + \pi$ and $\Omega \to \Lambda + \mathrm{K} \to p + \mathrm{K} + \pi$. The transverse momentum spectra in different centrality classes are shown in Fig. 10. In order to extract particle yields integrated over the full p_T range, the spectra are fitted using the blast-wave parametrization [10]. Yields are calculated integrating the corrected spectra in the measured p_T range and extrapolating outside by means of the fit function. As discussed in detail in [21], the enhancements have been calculated

as the ratio between the yields in Pb–Pb collisions and those in pp interactions at the same energy, both normalized to the number of participants. The pp reference values were obtained interpolating ALICE data at two energies ($\sqrt{s} = 0.9$ and 7 TeV) for the Ξ and STAR data at $\sqrt{s_{NN}} = 200$ GeV and ALICE data at 7 TeV for the Ω. In Fig. 11(left panel) the enhancements as a function of the mean number of participants are shown (full symbols): they increase with centrality and with the strangeness content of the particle as already observed at lower energies. Comparing the ALICE measurements with those at SPS and RHIC (hollow symbols), the enhancements are found to decrease as the centre-of-mass energy increases, continuing the same trend established at lower energies and first observed at SPS. The measured yields of several hadrons normalized to the pion

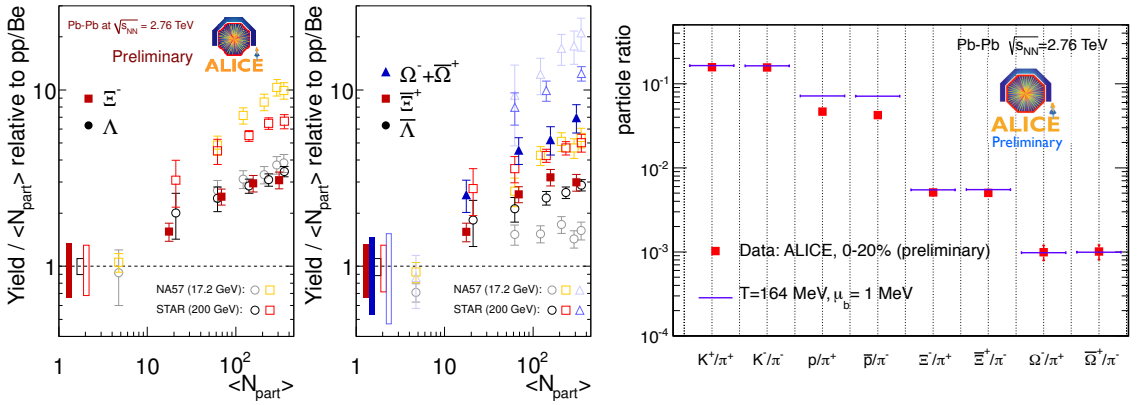

Figure 11: Left: strangeness enhancements in |y|<0.5 as a function of the mean number of participants N_{part} measured by ALICE and compared to SPS and RHIC data. The bars on the dotted line indicate the systematic uncertainties on the pp reference. Please note that the plots does not show the ALICE results for Λ and $\bar{\Lambda}$ Right: yields of several hadrons normalized to the pion yield in $0-5\%$ central collisions.

yield in $0-5\%$ central collisions can be compared to thermal model predictions as shown in Fig. 11 (right panel). With a temperature of $T_{ch} = 164$ MeV predicted by A. Andronic et al.[13] the model reproduces both kaon and multi-strange production but fails with protons. The same model can reproduce proton yields with an ad-hoc $T_{ch} = 148$ MeV, though multi-strange production is underestimated in this case.

5. Conclusions

The transverse momentum spectra of identified particles have been measured by the ALICE collaboration in pp collisions at $\sqrt{s} = 900$ GeV and 7 TeV and in Pb–Pb collisions at $\sqrt{s_{NN}} =$ 2.76 TeV. Proton–proton results do not show any evident $\sqrt{s}$ dependence in hadron production ratios. In Pb–Pb collisions the average transverse momenta and the fits to the spectral shapes indicate a $\approx 10\%$ stronger radial flow than at RHIC energies. The ratio between the anti-proton and π^- production yields is significantly lower than statistical model predictions, considering a chemical freeze-out temperature $T_{ch} = 160-170$ MeV. Multi-strange baryon spectra in Pb–Pb interactions were measured up to $p_T = 9$ GeV/c for the most central events. The enhancements in the strangeness content have been also measured in four centrality classes: they increase with centrality following the hierarchy based on the strangeness content of the particle. The comparison

with lower energy data shows that the enhancements decrease with increasing energy as already observed at SPS and between SPS and RHIC.

References

[1] B. Muller and J. L. Nagle, Ann.Rev.Nucl.Part.Sci. 56, 93 (2006), arXiv:0602029 [nucl-th].

[2] Tetsufumi Hirano, Pasi Huovinen, Yasushi Nara, Phys.Rev. C84 (2011)

[3] E. Scomparin (ALICE Collaboration), these proceedings

[4] ALICE Collaboration, J. Phys. G32, 1295 (2006)

[5] ALICE Collaboration, J. Instrum. 3, S08002 (2008)

[6] C. Tsallis, J. Stat. Phys. 52, 479 (1988)

[7] ALICE Collaboration, Eur. Phys. J. C71, 1655 (2011)

[8] ALICE Collaboration, Eur. Phys. J. C71, 1594 (2011)

[9] ALICE Collaboration, Phys. Rev. Lett. 106, 032301 (2011)

[10] E. Schnedermann, J. Sollfrank and U. Heinz, Phys. Rev. C48, 2462 (1993)

[11] M. Chojnacki (ALICE collaboration), Quark Matter 2011 conference proceedings, J.Phys.G38:124163,2011.

[12] J. Cleymans et al., Phys. Rev. C74, 034903 (2006)

[13] A. Andronic et al., Phys. Lett. B673, 142 (2009)

[14] STAR Collaboration, Phys. Rev. C79, 034909 (2009)

[15] PHENIX Collaboration, Phys. Rev. C69, 034909 (2004)

[16] BRAHMS Collaboration, Phys. Rev. C72, 014908 (2005)

[17] M. Floris (ALICE Collaboration), Quark Matter 2011 conference proceedings, J.Phys.G38:124163,2011.

[18] C. Shen, U. Heinz, P. Huovinen and H. Song, nucl-th/1105.3226

[19] R. Snellings (ALICE Collaboration), Quark Matter 2011 conference proceedings, J.Phys.G38:124163,2011.

[20] Song H., Bass S. A. and Heinz U.,Phys. Rev. C 83, 024912 (2011), nucl-th/1012.0555

[21] M. Nicassio (ALICE Collaboration), 2011 conference proceedings, Acta Physica Polonica B Proceedings Supplement Vol. 5 (2012), 237-242.